Long-chain alkenones in the Shimosa Group reveal palaeotemperatures of the Pleistocene interglacial Palaeo-Tokyo Bays

Hiroto Kajita[1,2,3,4]* , Tsutomu Nakazawa[2], Masayuki Utsunomiya[2], Naohiko Ohkouchi[3], Miyako Sato[3], Naomi Harada[3] and Hodaka Kawahata[4]

Abstract: The Shimosa Group, a Middle- to Late-Pleistocene sedimentary succession, has been the focus of stratigraphic attention because it lies beneath the Tokyo metropolitan area of central Japan. It is also of palaeoclimatic significance because it contains important interglacial marine strata of the past 450,000 years. Because the marine strata of the Shimosa Group were formed in the shallow inner bay known as the Palaeo-Tokyo Bay, rare occurrences of planktonic foraminifera make it difficult to quantitatively reconstruct the palaeo-sea surface temperatures (SSTs). Here, we extracted long-chain alkenones (LCAs) from the core GS-UR-1 penetrating the Shimosa Group to Marine Isotope Stage (MIS) 11. We found that the alkenone unsaturation ratio appears to reflect the SST of the Palaeo-Tokyo Bay formed during the peaks of MISs 5e, 7e, 9, and 11, which was consistent with the inflowing water mass changes inferred from the benthic foraminiferal assemblages. The palaeo-SSTs during each interglacial period were 2–3 °C higher than the pre-industrial levels of Tokyo Bay and seemed to reach a level similar to that of the Holocene thermal maximum. The findings of this study demonstrate that the LCA-based proxy, which has not before been utilised in studies on the Shimosa Group, has strong potential to provide palaeoceanic and stratigraphic information.

Keywords: Alkenone palaeothermometer, Interglacial periods, Shimosa Group

1 Introduction

Modern increases in greenhouse gas concentrations in the atmosphere and the weather catastrophes in recent years have stimulated growing public and scientific interest. Palaeotemperature reconstructions for past interglacial periods are particularly important in palaeoenvironmental studies because they provide a basis for comparison with the present interglacial period (Holocene) and its future evolution under the influence of global warming (Tzedakis et al. 2009, 2012). Of particular importance is the last 450,000 years, when the 100-kyr eccentricity cycle characterising modern climate was established (the so-called mid-Brunhes event) because some of the interglacial periods during this era are characterised by relatively high atmospheric CO_2 concentrations and have potentially been warmer than the present day (e.g. Droxler et al. 2003; Lüthi et al. 2008; Melles et al. 2012; Uemura et al. 2018). The latest Intergovernmental Panel on Climate Change report states that the last interglacial period, Marine Isotope Stage (MIS) 5e, was 0.5–1.5 °C higher in surface temperature than the pre-industrial period when assessed on a global average and had a warmer environment approaching the current greenhouse effect on Earth (Six Assessment Report 2021). However, there are large diversities among these interglacial periods in terms of the regional variation in their intensity, which makes their climatic structure and controlling mechanism elusive (Lang and Wolff 2011;

*Correspondence: kajita322@frontier.hokudai.ac.jp
[1] National Institute of Polar Research, Research Organization of Information and Systems, 10-3 Midori-tyo, Tachikawa, Tokyo 190-8518, Japan
Full list of author information is available at the end of the article

Milker et al. 2013; Otto-Bliesner et al. 2013; Hoffman et al. 2017; Turney et al. 2020).

The climate in central Honshu Island, Japan, is controlled by unique oceanic conditions (Fig. 1a). It faces the Kuroshio extension and subarctic fronts, which generate a distinct sea surface temperature (SST) gradient in the latitudinal direction (Kida et al 2016). It is also located near the northern limit of the westerly jet that bounds the East Asian summer monsoon front, where temperatures and precipitation vary greatly at its boundaries (Sampe and Xie 2010; Nagashima et al. 2013; Tada and Murray 2016). Because of these oceanic and atmospheric conditions, the north–south anomaly in the climate of Honshu Island is extremely large, meaning that it is sensitive to global climate change, and relatively large signals of palaeoclimatic and palaeoceanic changes at various chronological scales have often been observed (e.g. Haneda et al. 2020; Kajita et al. 2020b).

Despite their high palaeoclimatic significance, few geological samples can be used for systematic and continuous palaeotemperature reconstructions for multiple interglacial periods after the mid-Brunhes event. Continuous and accurately dated archives, such as lake and marine sediments, are promising to provide comprehensive information. In the case of lakes, the sediment core recovered from Lake Biwa, the largest and oldest lake in Japan, has been recorded to be up to approximately 450,000 years old, and provides palaeoclimate information based on pollen indicators (Nakagawa et al. 2008; Tarasov et al. 2011). With respect to marine sediment cores, except for some sediment cores drilled in the Japan Sea and the East China Sea on Integrated Ocean Drilling Program (IODP) Expedition 346 (Tada et al. 2018; Sagawa et al. 2018; Clemens et al. 2018) and off the Shimokita Peninsula on D/V CHKYU CK06-06 (trial voyage for IODP Expeditions) (Phillips and Harwood 2017), there are a few promising archives, particularly on the Pacific side.

In this study, we focused on marine strata situated in the subducting coastal plains formed during past sea-level highstands. Typical examples are distributed in the Osaka and Kanto Plains, which are called the Osaka Group and Shimosa Group, respectively (Masuda 2007). They are characterised by the cyclic deposition of shallow-marine and terrestrial strata related to

glacial–interglacial sea-level changes during the Middle to Late Pleistocene. Previous palaeoenvironmental studies using pollen-based proxies have provided important information on climate change during past interglacial periods (e.g. Okuda et al. 2002; Kariya et al. 2010; Kitaba et al. 2013). However, information on the marine environment, especially quantitative palaeo-SSTs, is scarce because of the few occurrences of planktic foraminifera in these successions.

Here, we found that organic biomarkers, long-chain alkenones (LCAs), are preserved in the marine strata of the Shimosa Group. LCAs are composed of C_{35}–C_{42} unsaturated methyl and ethyl ketones with two to four double bonds and feature unique lipid biomarkers produced by Isochrysidales haptophytes inhabiting sea surface waters (Volkman et al. 1980; Marlowe et al. 1984), brackish-saline lakes (Theroux et al. 2010; Plancq et al. 2019), freshwater lakes (Theroux et al. 2010; Longo et al. 2018; Richter et al. 2019), and sea ice (Wang et al. 2021). Based on culture experiments, it has been confirmed that the degree of unsaturation in LCAs is strongly correlated with the growth in temperature of haptophytes (Prahl et al. 1988; Sawada et al. 1996; Nakamura et al. 2014; Araie et al. 2018). In marine settings, except where large freshwater inflows or sea ice are distributed, the degree of unsaturation in C_{37} methyl ketones, which mostly originate from pan-global *Gephyrocapsa* spp. (including *G. huxleyi* formerly known as *Emiliania huxleyi*), can be used as palaeo-SST proxies (Müller et al. 1998; Tierney and Tingley 2018). Using this palaeotemperature proxy, we attempted to quantitatively reconstruct the SSTs during the MISs 5e, 7e, 9, and 11 that were recorded in the Shimosa Group.

2 Geological setting
The Kanto Plain, which covers the Tokyo metropolitan area of Japan, was formed as part of the tectonic basin developed in response to the subduction of the Pacific and Philippine Sea Plates beneath the North American Plate. This tectonic setting has resulted in a continuously subsiding basin with an uplifting and tilting margin relative to the basin centre. The Kanto tectonic basin is now buried with Neogene to Quaternary sediments up to 3,000 m thick, forming the widest plain (ca. 17,000 km[2]) in Japan (Suzuki 2002). The present-day Kanto Plain

---

(See figure on next page.)

Fig. 1 Maps showing the overall setting of the drill site of core GS-UR-1. **a** The marine and atmospheric environment around the Japanese islands, including the study site, is shown in this figure. The blue and red arrows represent the paths of the Oyashio and Kuroshio currents. The core sites referred to in this study are also shown. This base map was generated using Generic Mapping Tools. (b) Topography and geology around the core site. The sampling location of the core KT12-06-2B (Kajita et al. 2020b) is also shown. The base map was generated using the Seamless Digital Geological Map of Japan (Geological Survey of Japan, AIST 2020)
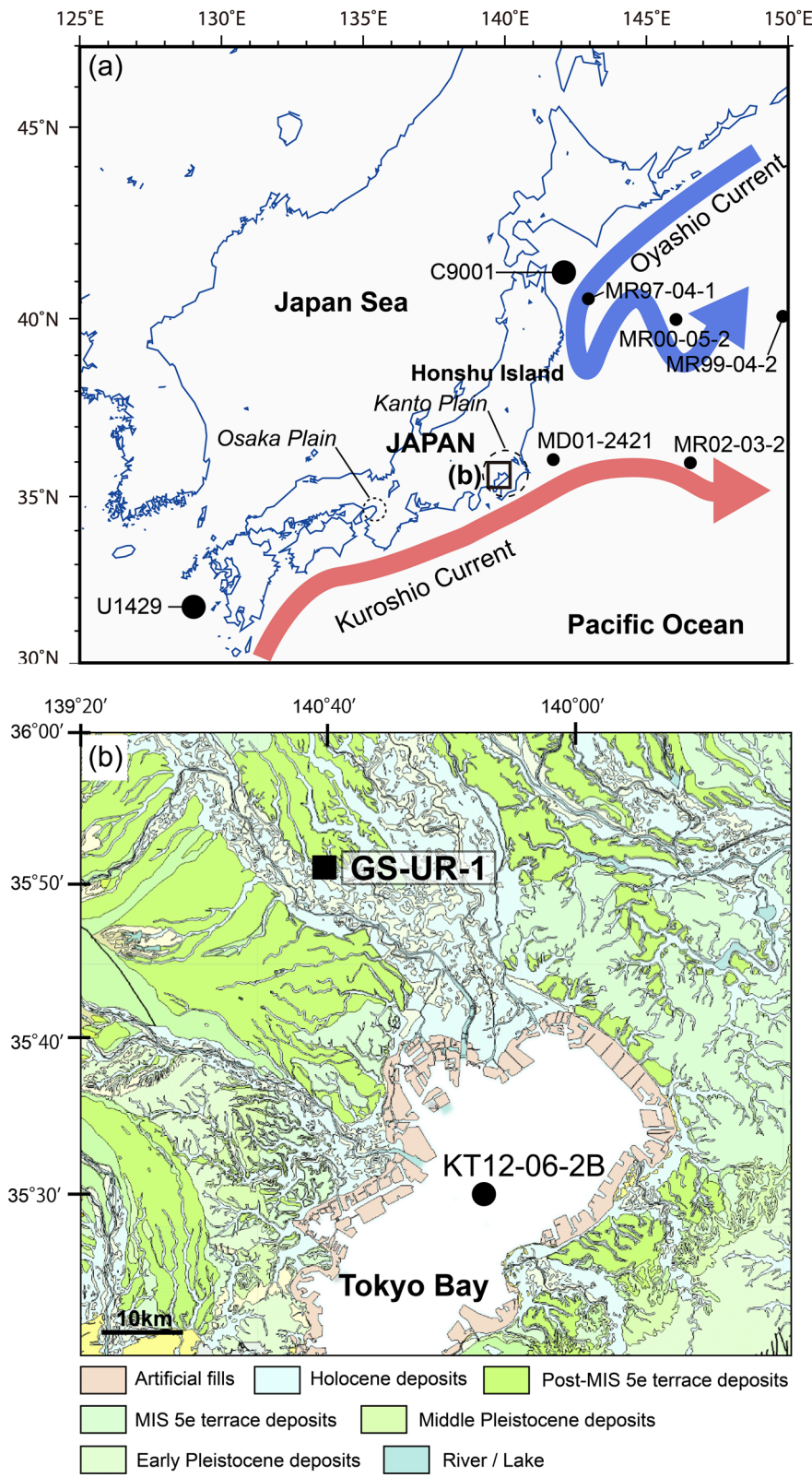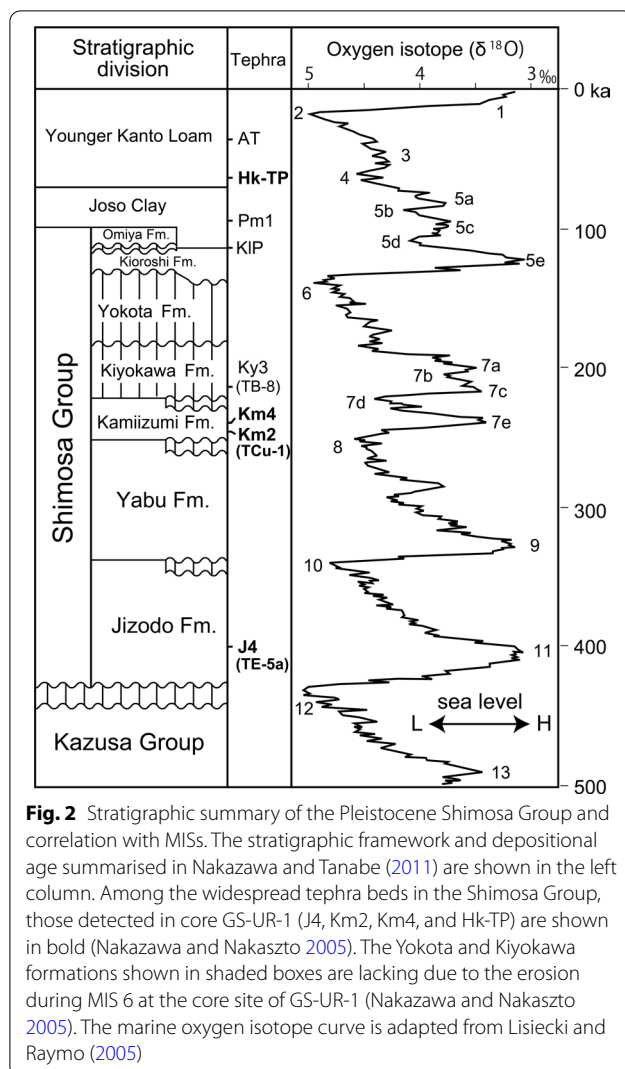
Fig. 1 (See legend on previous page.)

Kajita *et al. Progress in Earth and Planetary Science*   (2022) 9:40

Page 4 of 13

Fig. 2 Stratigraphic summary of the Pleistocene Shimosa Group and correlation with MISs. The stratigraphic framework and depositional age summarised in Nakazawa and Tanabe (2011) are shown in the left column. Among the widespread tephra beds in the Shimosa Group, those detected in core GS-UR-1 (J4, Km2, Km4, and Hk-TP) are shown in bold (Nakazawa and Nakaszto 2005). The Yokota and Kiyokawa formations shown in shaded boxes are lacking due to the erosion during MIS 6 at the core site of GS-UR-1 (Nakazawa and Nakaszto 2005). The marine oxygen isotope curve is adapted from Lisiecki and Raymo (2005)

is underlain by the Middle to Late Pleistocene Shimosa Group, which consists of fluvial–coastal depositional cycles (Tokuhashi and Kondo 1989) related to sea-level changes from MIS 12 to 5e (Nakazato and Sato 2001). The marine strata heavily accumulated in the Kanto Plain (Palaeo-Tokyo Bay), when the relative sea level increased during each interglacial period. They can be subdivided into the Jizodo, Yabu, Kamiizumi, Kiyokawa, Yokota, and Kioroshi formations in ascending order and are bounded by a discontinuity formed during the sea-level lowstands (Tokuhashi and Endo 1984; Nakazawa and Nakaszto 2005; Nakazawa et al. 2006; Nakazawa and Tanabe 2011) (Fig. 2). The Kiroshi Formation, which was deposited during the last interglacial period (MIS 5e), can be observed in the shallow subsurface part of the upland areas that have not been subjected to fluvial erosion since the latest Pleistocene (Fig. 1b).

3 Materials and methods

3.1 Core GS-UR-1

The sediment core GS-UR-1 was obtained from Saitama City, Saitama Prefecture, in the Omiya Upland (139°39′25″ E, 35°51′13″ N) from an elevation of 16.29 m (Fig. 1b). This core was drilled in 2004 and stored at room temperature until our analysis. The core was recovered using a triple-tube sampler with a diameter of 116 mm and a total length of 101.95 m. The stratigraphy and depositional age of GS-UR-1 have been described comprehensively by Nakazawa and Nakazato (2005) and are outlined below.

The core comprises five depositional cycles bounded by unconformities formed at sea-level lowstands. The cycles are composed of non-marine and marine beds accumulated under the influence of sea-level change, except for the fluvial terrace deposits and the surface soil of the shallowest cycle. These depositional cycles in GS-UR-1 are correlated with the Jizodo, Yabu, Kamiizumi, and Kioroshi formations of the Shimosa Group in ascending order, based on the sea-level change inferred from the depositional cyclicity and intercalated with several marker tephra beds. These marker tephra beds, J4 (TE-5a), Km2 (TCu-1), Km4, and Hk-TP, were detected in GS-UR-1 (Fig. 2). Of these, J4 (TE-5a) is recognised in the marine bed of the lowest cycle in GS-UR-1. It is known as a marker tephra bed of the Jizodo Formation (Tokuhashi and Endo 1984) and is correlated with A_1Pm and Ty1 tephras (Nakazawa et al. 2009) intercalated at the stratigraphic level during or immediately following the peak of MIS 11 (Kameo et al. 2006; Tsukamoto et al. 2007; Ito and Danišík, 2020) (Fig. 2). These results indicate that the lowest cycle of GS-UR-1 corresponds to the Jizodo Formation of MIS 11. Km2 (TCu-1) and Km4 are intercalated in a brackish/marine bed at two cycles above the Jizodo Formation in GS-UR-1. They are known as marker tephra beds of the Kamiizumi Formation (Tokuhashi and Endo 1984). The Km2 tephra is widespread in the Kanto Plain (Naya et al. 2020), and believed to indicate the early MIS 7e (Nakazato and Sato 2001; Naya et al. 2020). This indicates that the depositional cycle intercalating Km2 and Km4 in GS-UR-1 corresponds to the Kamiizumi Formation of MIS 7e and that the cycle between the Jizodo and Kamiizumi formations is correlative to the Yabu Formation of MIS 9. Hk-TP is known as a tephra bed indicating MIS 4 (66.0 ± 5.5 ka: Aoki et al. 2008) and is intercalated at the base of the surface soil overlying the fluvial terrace deposits in the shallowest part of GS-UR-1. Therefore, the depositional cycles of marine beds below the fluvial terrace deposits seem to correlate with the Kioroshi Formation of MIS 5e.

Based on the tephra beds described above and comparing them with the stratigraphy in the stratotype of the

Kajita *et al. Progress in Earth and Planetary Science* (2022) 9:40

Page 5 of 13

Shimosa Group, the Jizodo (deposited in MIS 11), Yabu (MIS 9), Kamiizumi (MIS 7e), and Kioroshi (MIS 5e) formations were identified in the core GS-UR-1. Of these, the Yabu, Kamiizumi, and Kioroshi formations can be divided into lower and upper parts, respectively, with bay ravinement surfaces. While the lower parts are composed mainly of fluvial gravels and mud containing plant rootlets, the upper parts consist of inner-bay sediments with abundant marine microfossils. Such facies stacking patterns suggest a rising sea level and transgression during each interglacial period.

Benthic and planktic foraminiferal assemblages were also analysed for core GS-UR-1 (Kaneko et al. 2018). In that study, a maximum of 20 g sediment was sampled from 98 levels covering almost the entire span of Jizodo, Yabu, Kamiizumi, and Kioroshi formations. The sediments were disaggregated by boiling and then washed with a sieve with a mesh size of 0.074 mm. For specular examination, the residue was divided so that the foraminifera population reached 200, and individuals larger than 0.125 mm were selected for identification. Although a few foraminifers were detected from the lower part of the Kioroshi Formation and none from the lower parts of the Kamiizumi or Yabu formations, the marine bed above the bay ravinement surface of each formation yielded enough benthic foraminiferal fossils for palaeoenvironmental analysis, whereas the number of planktic foraminifera was less than 20 individuals/g at maximum, probably due to the shallow inner-bay environments.

3.2 Organic geochemical analysis
In this study, we obtained silty to sandy mud samples from stratigraphic levels similar to those of the foraminiferal analysis (Kaneko et al. 2018) and carried out an organic geochemical analysis following the procedures of Ohkouchi et al. (2005). Approximately 6 g of the dried sediment were crushed into a fine powder, and lipids were extracted by sonification using a mixed solvent of dichloromethane/methanol (70:30, v/v). The lipids were saponified with 0.5 M KOH in MeOH. The saponified samples were then extracted with n-hexane to obtain the neutral components. The neutral lipids were separated into four sub-fractions by silica gel column chromatography. The N-1 fraction (hydrocarbons) and N-2 fraction (ketones, esters, and aldehydes) were extracted using a solvent mixture of n-hexane and dichloromethane. For the identification of LCAs by gas chromatography (GC), the N-2 fraction was introduced into an Agilent Technologies (Santa Clara, CA) model 7890A gas chromatograph connected to a mass-selective detector with a non-polar VF-5 ms fused silica column (J&W Scientific, 30 m/0.25 mm

internal diameter 5% phenyl-dimethylpolysiloxane liquid phase) and an Instant Connect Programmable Temperature Vaporizing Injector (Thermo Fisher Scientific). Helium was used as the carrier gas, and the column flow rate was 36 cm s^{-1}. The oven temperature was programmed with an initial temperature of 40 °C (held for 2 min), which was increased at 30 °C min^{-1} to 120 °C and then at 6 °C min^{-1} to 320 °C (held for 20 min). The samples were dissolved in 50 μL of hexane, of which 1 μL was injected. The detection limit of LCAs was 0.8 ng, which was estimated by repeated injection of the external standard of 2-nonadecanone. The samples in which LCAs were detected were then quantified using an Agilent Technologies (Santa Clara) model 6890A GC with a flame ionisation detector (FID) using mid-polar VF-200 ms fused silica columns (J&W Scientific, 60 m/0.25 mm internal diameter, trifluoropropylmethylsiloxane lipid phase), which exhibited adequate LCA separation (Longo et al. 2013). Hydrogen was used as the carrier gas, and the column flow rate was maintained at 36 cm s^{-1}. The oven temperature was then programmed with an initial temperature of 60 °C (held for 1 min), which was increased at 20° C min^{-1} to 250 °C (held for 48 min), and then at 20 °C min^{-1} to 310 °C (held for 15 min). The samples were dissolved in 10–50 μL of hexane, of which 3 μL was injected. The detection limit of LCAs was 1.4 ng, which was estimated by the repeated injection of the external standard of 2-nonadecanone.

3.3 Identification of coccolithophores
To detect *Gephyrocapsa* spp., which is an ocean-dwelling LCA producer, sandy mud samples collected from each of the Jizodo, Yabu, Kamiizumi, and Kioroshi formations were suspended in tap water by gentle ultrasonication and then collected on a membrane filter with a pore size of 0.45 μm (HAWP04700, Millipore); subsequently, the samples were dried for 12 h in a desiccator. The filters (approximately 5 × 5 mm) containing the dried samples were mounted onto the stub of a scanning electron microscope (SEM) (JSM-6390LV, JEOL) coated with gold and gold–palladium using an E-1020 sputter coater (Hitachi High-Tech) for further observation.

4 Results
GC-mass spectrometry (MS) analysis showed that LCAs were preserved in almost all the marine strata where foraminiferal shells were found, whereas they were not detected in strata without foraminiferal shells. In most samples with LCAs, major components (C_{37}–C_{39} unsaturated methyl and ethyl ketones with 2–3 double bonds) were quantified from GC chromatograms and then $U^{K'}_{37}$

values (defined as $= [C_{37:2}Me]/[C_{37:2}Me] + [C_{37:3}Me]$, where $[C_{37:2}Me]$ and $[C_{37:3}Me]$ represent the concentrations of di-unsaturated and tri-unsaturated C_{37} methyl ketones, respectively) were obtained (Fig. 3, Additional file 1: Table S1). However, in some cases, reliable $U_{37}^{K'}$ values could not be obtained because of the small peak intensities or the co-elution of other substances on the GC chromatogram.

The SEM images of each marine strata showed that the stratigraphic levels with high LCA concentrations contained *Gephyrocapsa* coccoliths (Fig. 4). *Gephyrocapsa* coccoliths (4.0–5.5 μm long) with a bridge at a high angle to long axis were assigned as *G. oceanica* following the biometric subdivision of Young et al. (2003). This species was detected in the Yabu (MIS 9), Kamiizumi (MIS 7e), and Kioroshi (MIS 5e) formations. Small (< 3 μm) placolith specimens from the Kioroshi Formation included gephyrocapsids, which lacked a bridge (probably assigned as *G. huxleyi*), and *Gephyrocapsa* sp. 1 (Fig. 4). Medium-sized (3.0–4.0 μm long) *Gephyrocapsa* coccoliths detected from the Yabu Formation with a bridge at a low angle to the long axis were assigned as *Gephyrocapsa* sp. 2. Further, *Gephyrocapsa* sp. 1 and 2 resembled *G. ericsonii* and *G. muellerae*, respectively, but these morphotypes were not assigned as extant species based on our sporadic morphometric data, considering their complicated phylogenetic relation in the Late Pleistocene (Bendif et al. 2019). In the Jizodo Formation (MIS 11), coccoliths were dissolved, but coccoliths of *Gephyrocapsa* spp. with bridges were detected.

5 Discussion
5.1 Assessment of the $U_{37}^{K'}$-SST
In this study, we showed for the first time that LCAs are preserved in the marine strata of the Shimosa Group. $U_{37}^{K'}$-SST is a useful tool for reconstructing quantitative palaeotemperatures in the coastal shallow sea because *Gephyrocapsa* spp., which specifically synthesises LCAs in marine settings, reproduce even in coastal and inland bay environments (e.g. Kawahata et al. 2009; Kajita et al. 2018). In low salinity seas, LCAs have been potentially synthesised by other Isochrysidaceae haptophytes living in brackish water that have characteristics different from those of *Gephyrocapsa* spp. (e.g. Salacup et al. 2019; Kaiser et al. 2019). Based on field and culture studies, most of these are characterised by the abundant synthesis of $C_{37:4}Me$ and extremely low $C_{38:2}Me$ and $C_{38:3}Me$ (Nakamura et al. 2014; Araie et al. 2018; Plancq et al. 2019; Zheng et al. 2019; Kajita et al. 2020a; Huang et al. 2021; Yao et al. 2022). In all samples where $U_{37}^{K'}$ was calculated in this study, no distinct peak of $C_{37:4}Me$ was detected, and C_{38} alkenones with a methyl group were detected (Fig. 3, Additional file 1: Table S1). *Gephyrocapsa*

coccoliths were detected in all formations in the Shimosa Group in this study (Fig. 4), and these have also been detected in the present-day Tokyo Bay (Ogura and Sato 2001). Therefore, LCAs in the marine strata of the Shimosa Group are likely to be derived mostly from *Gephyrocapsa* spp.

Palaeo-SSTs of only samples with good chromatograms were calculated from $U_{37}^{K'}$ based on the culture experiments of *G. oceanica*, which was isolated from the inner bay of Japan (Sawada et al. 1996), using the following conversion formula:

$$SST(°C) = (U_{37}^{K'} + 0.204)/0.044$$

As the evolutionary characteristics of extant *Gephyrocapsa* spp. after 600 ka are complex (Bendif et al. 2019), the following global core-top calibration formula, which is empirically applicable to Quaternary sediment based on comparisons with data from other SST proxies (McClymont et al. 2005), was also used to calculate palaeo-SSTs (Müller et al. 1998):

$$SST(°C) = (U_{37}^{K'} + 0.044)/0.033$$

In the present-day Tokyo Bay, the $U_{37}^{K'}$-SST of the surface sediment is approximately 2 °C higher than the measured annual mean SST (Kajita et al. 2020b). Therefore, we discuss that the $U_{37}^{K'}$-SSTs recovered in this study may reflect the temperature range from annual mean to summer temperatures of Palaeo-Tokyo Bays.

It is expected that the LCAs have been well-preserved because of the small degeneracy of the Shimosa Group, meaning it has not been subjected to strong compaction or diagenesis since the time of deposition (Nakazawa and Nakazato 2007). Well-preserved LCAs have also been detected in the underlying Kazusa Group, which
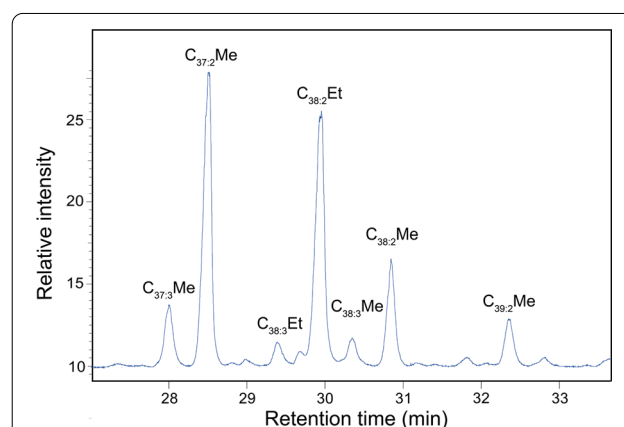

Fig. 3 Partial GC chromatogram of LCAs detected from the core GS-UR-1. The sample depth was 99.38–99.40 m, corresponding to the Jizodo Formation
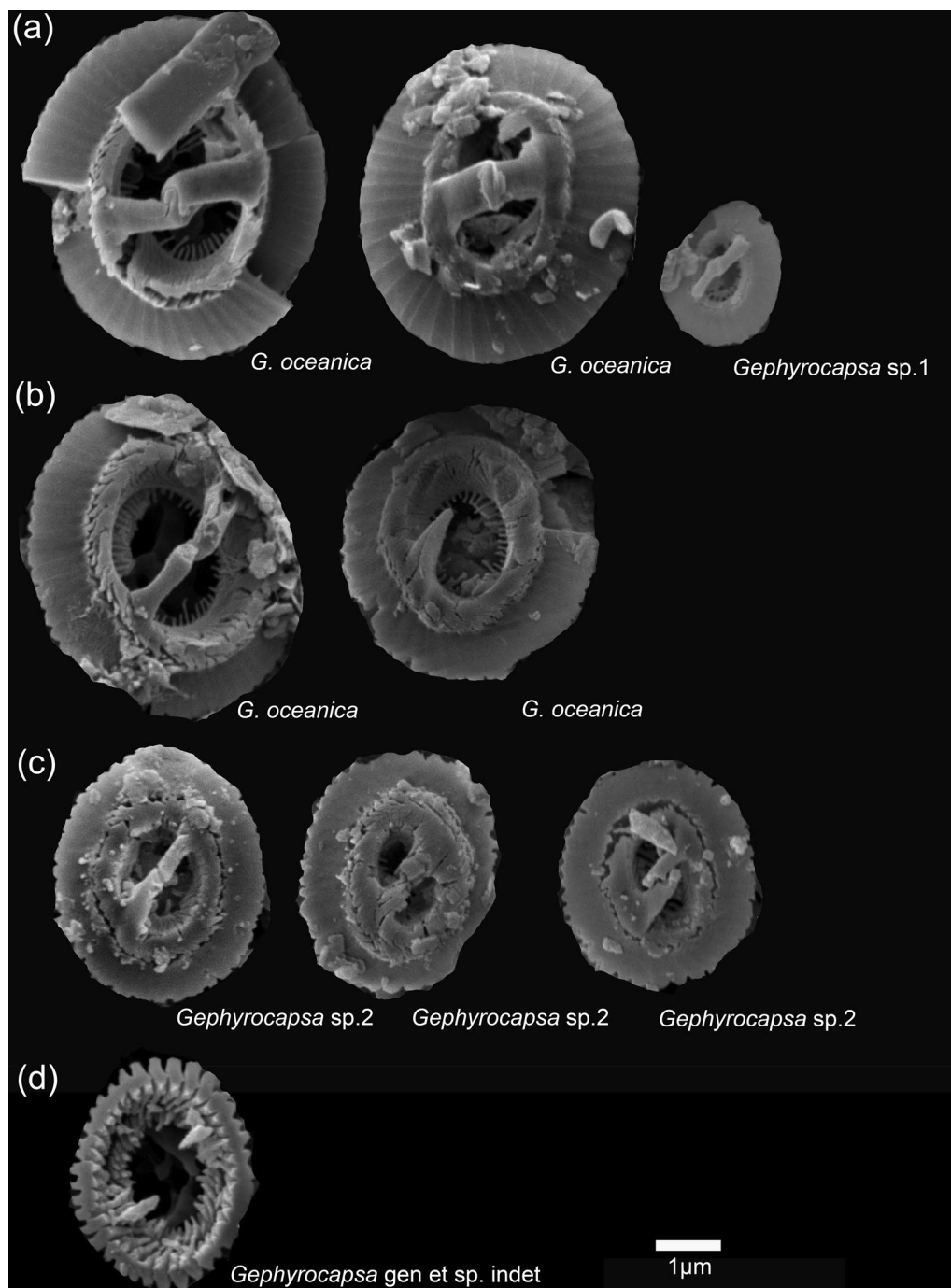
Fig. 4 SEM images of *Gephyrocapsa* spp. obtained from core GS-UR-1. **a** *G. oceanica* and *Gephyrocapsa* sp. 1 obtained from a sample collected at a depth of 29.20–29.22 m in the Kioroshi Formation. **b** *G. oceanica* obtained from a sample collected at a depth of 52.78–52.80 m in the Kamiizumi Formation. **c** *Gephyrocapsa* sp. 2 obtained from a sample collected at a depth of 77.25–77.27 m, corresponding to the Yabu Formation. **d** *Gephyrocapsa* gen et sp. indet obtained from a sample collected at a depth of 101.7–101.9 m in the Jizodo Formation

has experienced a deeper burial depth than the Shimosa Group (Kajita et al. 2021). In the following sections, we discuss the palaeotemperature variations during each interglacial period, especially in relation to foraminiferal production proposed by Kaneko et al. (2018).

Kajita *et al. Progress in Earth and Planetary Science*   (2022) 9:40

Page 8 of 13

5.2 Comparison with the foraminifer assemblages

The stratigraphic levels, at which LCAs were detected, are almost the same as those having a high relative abundance ratio of planktonic foraminifera to benthic foraminifera (P/T ratio) (Kaneko et al. 2018). Both the number of planktonic foraminifera per sediment weight and P/T ratio are positively correlated with distance from the shoreline (Gibson 1989). Therefore, when the transgressions in the Palaeo-Tokyo Bays were sufficiently advanced, LCA producers were dominant at the core site (Fig. 5). Although benthic foraminiferal assemblages can be used as indicators of the marine environment in Palaeo-Tokyo Bay, the corresponding information obtained from these assemblages is limited as it is qualitative (Kaneko et al. 2018). Here, we compare quantitative $U_{37}^{K'}$-SSTs with the benthic foraminiferal assemblages for the strata in which the total number of benthic foraminifera reached 200 individuals, which is a common requirement for environmental change analysis (Fig. 5). We focused on the production of species that are relatively abundant in the core, that is, *Ammonia japonica*, *Pseudorotalia gaimardii* (*Rotalinoides gaimardi*), *Buccella frigida*, and *Elphidium clavatum*. Many of these species can also be found in present-day Tokyo Bay (Kosugi et al. 1991). Of them, *A. japonica* and *P. gaimardii* are found in a wide range of areas along the coast of Japan but indicate a relatively warm water environment, including that of the Kuroshio Current (Hasegawa 1993). In contrast, *B. frigida* and *E. clavatum,* which are abundant in subarctic neritic faces under the influence of Oyashio Current water (Ishiwada 1964; Hasegawa 1993), suggest a relatively colder environment. The benthic foraminiferal assemblage is influenced not only by water temperature but also by the nutrient and redox environment of the sea floor (Murray 2001); however, it is the rare proxy that provides information on continuous marine environmental change from the Shimosa Group. These fluctuations broadly support the $U_{37}^{K'}$-SST changes (Fig. 6); therefore, we believe that $U_{37}^{K'}$-SSTs in the Shimosa Group are robust and provide quantitative palaeotemperatures which may be related to water mass structures between the Kuroshio and Oyashio currents.

5.3 Interglacial environments of (Palaeo-) Tokyo Bays

The examined samples were obtained from the marine strata formed during the sea-level highstands of MIS 5e, 7e, 9, and 11. Assuming that the maximum sea-level rise in the Palaeo-Tokyo Bay could be linked to global ice sheet volume fluctuations, the LCA-based palaeotemperatures can be interpreted as reflecting SSTs around the peak of each interglacial period. Within the marine strata of the Jizodo Formation, the key tephra bed of TE-5a accumulated during or immediately after the peak

of MIS 11 (Kameo et al. 2006; Tsukamoto et al. 2007; Ito and Danišík, 2020) can be recognised above the stratum level where LCAs are detected, which supports our interpretation. As for the Kioroshi Formation, the stratigraphic level near the bay ravinement surface is considered to correspond to the sea-level highstand of MIS 5e (Nakazawa et al. 2006) and abundant LCAs are detected. The lower part below the bay ravinement surface, with poor preservation of LCAs and foraminifera, seems to have been formed in a restricted inner-bay environment as incised-valley fills where the salinity was too low for oceanic plankton to thrive (Nakazawa et al. 2006).

$U_{37}^{K'}$-SSTs in each formation generally showed decreasing trends towards the upper section, which might indicate the SST decrease during and after each sea-level highstand. Although data were not available for the lower part of the Jizodo Formation, which was out of the core GS-UR-1, $U_{37}^{K'}$-SSTs suggested that the Palaeo-Tokyo Bays in each interglacial period seemed to reach similar SSTs around their sea-level highstand. These temperatures are 2–3 ℃ higher than the $U_{37}^{K'}$-SSTs of the pre-industrial level of Tokyo Bay recovered from the sediment core KT12-06-2B (Kajita et al. 2020b) and possibly equivalent to or warmer than the values of the Holocene thermal maximum (5–7 ka), which was previously estimated to be approximately 2 ℃ higher than that of the pre-industrial level (Matsushima and Ohshima 1974; Matsushima 1979). High temperatures in MIS 5e compared to the present level have also been recorded in several cores (MD01-2421, MR97-04–1, MR99-04–2, MR00-05–2, MR02-03–2) collected from the Kuroshio–Oyashio mixing zone (Yamamoto et al. 2004; Koizumi and Yamamoto 2010), the core from site U1429 in the East China Sea under the influence of the branched Kuroshio Current (Lee et al. 2021), and the core from site C9001 off the northern Honshu coastal region under the influence of the Oyashio Current (Phillips and Harwood 2017). In the high latitudes of the Northern Hemisphere, not only in the Pacific Ocean but also globally, 1–2 ℃ warmer SSTs than the pre-industrial level have been recorded for the peak of MIS 5e, which are considered to have been caused by high summer insolation and positive feedback related to ice distributions (Hoffman et al. 2017; Thomas et al. 2020; Turney et al. 2020). Accordingly, we consider that the north–south temperature gradient along the coast of Japan formed by the Kuroshio–Oyashio interfrontal zone should have been shifted more to the north than it is today, which causes the Japanese coastal region to be generally warm. Our results suggest that MIS 9 seems to be the warmest interglacial since the mid-Brunhes event. These tendencies are comparable to the temperature records from cores U1429 and C9001 (Phillips and Harwood 2017; Lee et al. 2021), the CO_2 record in
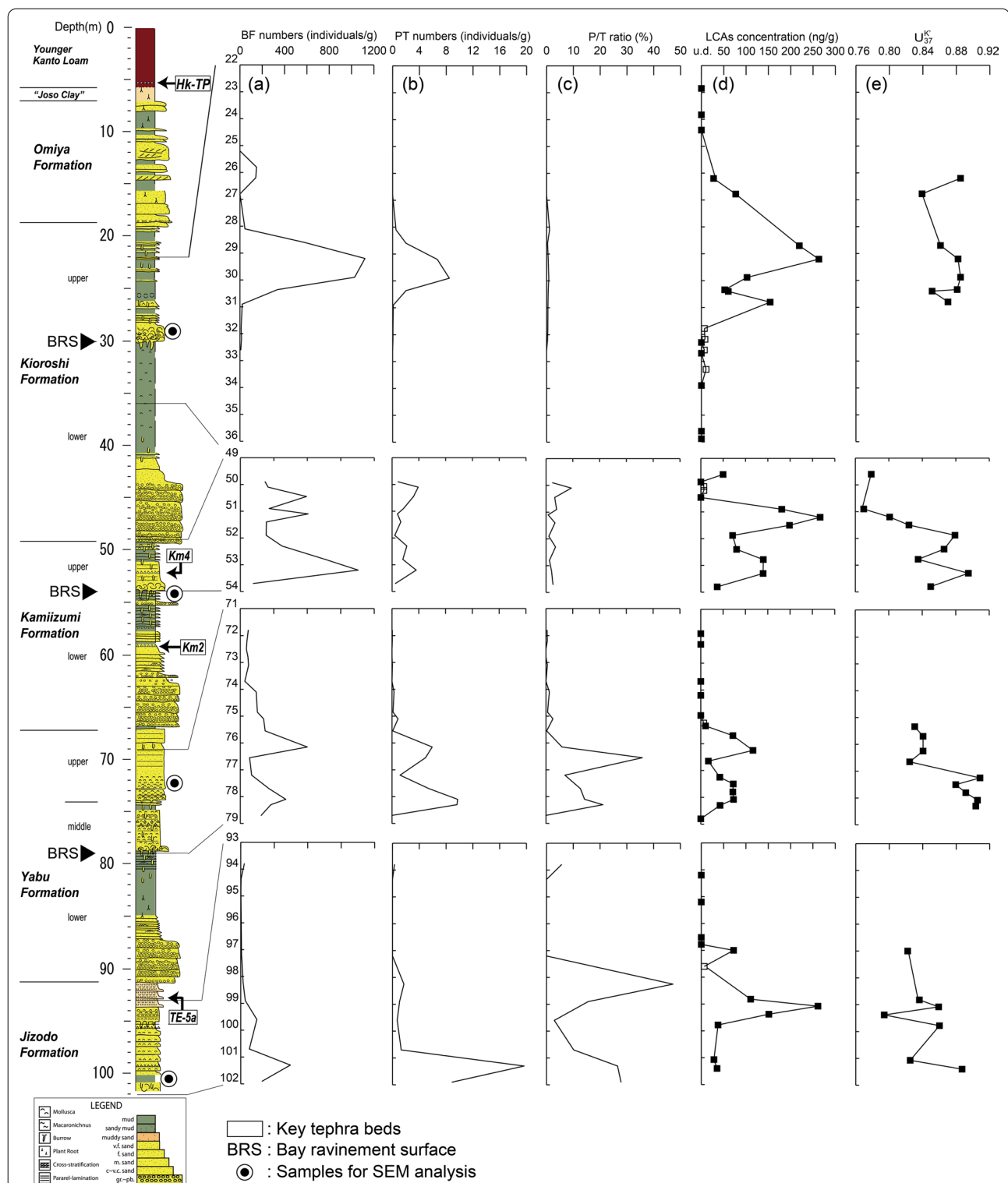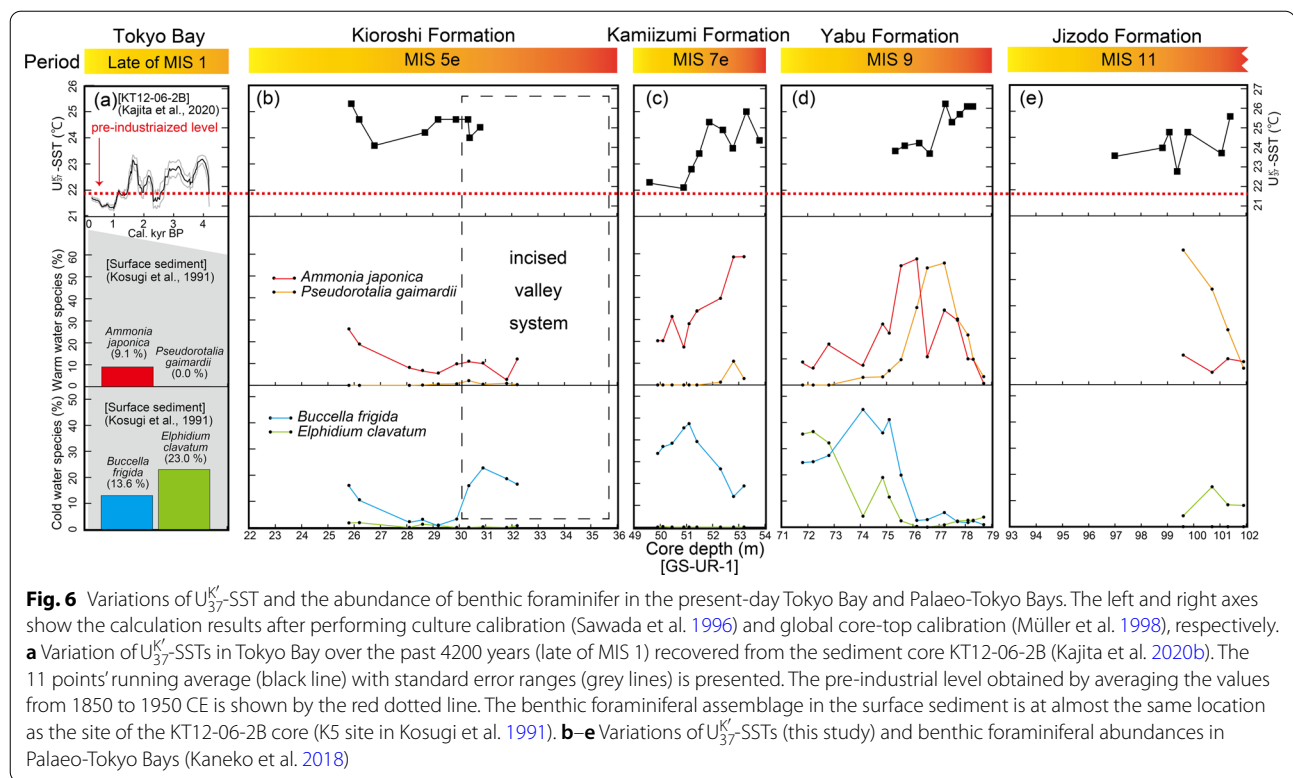
Fig. 5 Results of LCA concentration and $U_{37}^{K'}$-SST. The stratigraphic horizons examined in this study are shown in the left column with the columnar section of core GS-UR-1 described in Nakazawa and Nakazato (2005). **a–c** Variations in the total number of benthic and planktic foraminifera along with their relative abundance (P/T ratio) (Kaneko et al. 2018). **d–e** Variations in the LCA concentrations and $U_{37}^{K'}$-SSTs shown in this study. The white dots represent the samples in which LCAs were identified by GC/MS analysis, but clearly separated peaks could not be obtained by the GC chromatograph

Kajita *et al. Progress in Earth and Planetary Science*   (2022) 9:40

Page 10 of 13

Fig. 6 Variations of $U_{37}^{K'}$-SST and the abundance of benthic foraminifer in the present-day Tokyo Bay and Palaeo-Tokyo Bays. The left and right axes show the calculation results after performing culture calibration (Sawada et al. 1996) and global core-top calibration (Müller et al. 1998), respectively. **a** Variation of $U_{37}^{K'}$-SSTs in Tokyo Bay over the past 4200 years (late of MIS 1) recovered from the sediment core KT12-06-2B (Kajita et al. 2020b). The 11 points' running average (black line) with standard error ranges (grey lines) is presented. The pre-industrial level obtained by averaging the values from 1850 to 1950 CE is shown by the red dotted line. The benthic foraminiferal assemblage in the surface sediment is at almost the same location as the site of the KT12-06-2B core (K5 site in Kosugi et al. 1991). **b–e** Variations of $U_{37}^{K'}$-SSTs (this study) and benthic foraminiferal abundances in Palaeo-Tokyo Bays (Kaneko et al. 2018)

the Antarctic ice core (Uemura et al. 2018), and climate modelling results of past interglacial periods (Yin and Berger 2010). Therefore, we consider that interglacial SST variations in the Kuroshio–Oyashio boundary region including the Palaeo-Tokyo Bays have been linked to global climate changes via shifts in oceanic fronts.

5.4 $U_{37}^{K'}$-SSTs for stratigraphy of the Shimosa Group
The $U_{37}^{K'}$-SSTs revealed in this study provides useful information not only for palaeoclimatology but also for stratigraphic studies in the Shimosa Group, which is important for revealing the subsurface structure of the Kanto Plain, where the capital of Japan is located (Nakazawa et al. 2017). Because the sequences of the Shimosa Group are not always rich in interbedded key tephra beds, information on palaeoenvironmental changes mainly based on pollen assemblages has been used to estimate stratigraphic correlations between cores and outcrops in other regions (e.g. Nakazawa et al. 2006, 2017). However, pollen assemblages which have been preserved in coastal sediments do not always accurately reflect the local climate of the catchment area because of the wide variety of sedimentary processes involved (e.g. Igarashi et al. 2015). In addition, the quality of pollen-based palaeoenvironmental indices strongly depends on the current reference pollen dataset; therefore, care should be taken

when quantitatively comparing palaeorecords between different sites and periods (e.g. Tarasov et al. 2011). Compared to the pollen-based indices, $U_{37}^{K'}$-SST has the advantage that it can show similar variations in a wide range of contemporaneous strata. Consequently, $U_{37}^{K'}$-SST can be a new tool for elucidating the stratigraphy of the Shimosa Group and for extracting palaeoenvironmental information.

6 Conclusions
We detected LCAs in the marine strata of the Shimosa Group and succeeded in reconstructing the SSTs of Palaeo-Tokyo Bays formed during the past interglacial periods after the mid-Brunhes event. The $U_{37}^{K'}$ fluctuation in each interglacial formation was consistent with the water mass structure estimated from previously published benthic foraminiferal assemblages and seemed to indicate SST variations during those periods. $U_{37}^{K'}$-SSTs in the Palaeo-Tokyo Bays around the peak of MIS 5e, 7e, 9, and 11 were estimated to be 2–3 ℃ higher than the pre-industrial levels of Tokyo Bay with the highest temperature recorded in MIS 9. These characteristics were similar to the trends shown by previous studies of the surrounding ocean, suggesting that the $U_{37}^{K'}$-SST recorded in the Shimosa Group reflects the temperature variations associated with the shifts in the

Kajita *et al. Progress in Earth and Planetary Science*   (2022) 9:40

Page 11 of 13

northern limit of the Kuroshio Current during the past interglacial periods. This study demonstrates that LCAs can act as novel indicators that are useful for palae-oceanographic and stratigraphic studies in the Shimosa Group.

Abbreviations
IPCC: Intergovernmental Panel on Climate Change; LCAs: Long-chain alkenones; MIS: Marine Isotope Stage; SST: Sea surface temperature.

Supplementary Information
The online version contains supplementary material available at https://doi.org/10.1186/s40645-022-00499-y.

> **Additional file 1. Supplementary Table 1**. Abundance of LCAs in the core GS-UR-1.

Author contributions
HK proposed the research topic and designed the study. N.T. drilled the core and performed stratigraphic study. M.U. performed SEM analysis and identified coccoliths. HK carried out the geochemical experiments and wrote the manuscript. N.O., N.H., and HK organised the analytical devices and helped with the interpretations. M.S. assisted with the laboratory analysis. All authors have read and approved the final manuscript.

Availability of data and materials
The datasets supporting the conclusions of this article are included within the article and the additional file.

Declarations

Competing interests
The authors declare that they have no competing interests.

Author details
[1]National Institute of Polar Research, Research Organization of Information and Systems, 10-3 Midori-tyo, Tachikawa, Tokyo 190-8518, Japan. [2]Geological Survey of Japan, National Institute of Advanced Industrial Science and Technology, 1-1-1 Higashi, Tsukuba, Ibaraki 305-8567, Japan. [3]Japan Agency for Marine-Earth Science and Technology, 2-15 Natsushima, Yokosuka, Kanagawa 237-0061, Japan. [4]Atmosphere and Ocean Research Institute, The University of Tokyo, 5-1-5 Kashiwanoha, Kashiwa, Chiba 277-8564, Japan.

References
Aoki K, Irino T, Oba T (2008) Late Pleistocene tephrostratigraphy of the sediment core MD01-2421 collected off the Kashima coast, Japan. Quat Res (Daiyonki-Kenkyu) 47(6):391–407

Araie H, Nakamura H, Toney JL, Haig HA, Plancq J, Shiratori T, Leavitt PR, Seki O, Ishida K, Sawada K, Suzuki I, Shiraiwa Y (2018) Novel alkenone-producing strains of genus Isochrysis (Haptophyta) isolated from Canadian saline lakes show temperature sensitivity of alkenones and alkenoates. Org Geochem 121:89–103

Bendif EM, Nevado B, Wong ELY, Hagino K, Probert I, Young JR, Rickaby REM, Filatov DA (2019) Repeated species radiations in the recent evolution of the key marine phytoplankton lineage *Gephyrocapsa*. Nat Commun 10:4234

Clemens SC, Holbourn A, Kubota Y, Lee KE, Liu Z, Chen G, Nelson A, Fox-Kemper B (2018) Precession-band variance missing from East Asian monsoon runoff. Nat Commun 9(1):1–12

Droxler AW, Alley RB, Howard WR, Poore RZ, Burckle LH (2003) Unique and exceptionally long interglacial Marine Isotope Stage 11: Window into Earth warm future climate. Geophys Monogr Ser 137:1–14

Geological Survey of Japan, AIST (ed.) (2020) Seamless digital geological map of Japan 1: 200,000. June 9, 2020 version. Geological Survey of Japan, National Institute of Advanced Industrial Science and Technology

Gibson TG (1989) Planktonic benthonic foraminiferal ratios: Modern patterns and Tertiary applicability. Mar Micropaleontol 15:29–52

Haneda Y, Okada M, Kubota Y, Suganuma Y (2020) Millennial-scale hydrographic changes in the northwestern Pacific during marine isotope stage 19: Teleconnections with ice melt in the North Atlantic. Earth Planet Sci Lett 531:115936

Hasegawa S (1993) Distribution of recent benthic foraminifers as an indicator of thermal conditions of the seas around the Japanese Islands: An approach to reconstruction of Cenozoic oceanic condition. Fossils 55:17–33

Hoffman JS, Clark PU, Parnell AC, He F (2017) Regional and global sea-surface temperatures during the last interglaciation. Science 355(6322):276–279

Huang Y, Zheng Y, Heng P, Giosan L, Coolen MJ (2021) Black Sea paleosalinity evolution since the last deglaciation reconstructed from alkenone-inferred Isochrysidales diversity. Earth Planet Sci Lett 564:116881

Igarashi Y, Yamamoto M, Noda A, Ikehara K, Katayama H (2015) Deposition pattern and sources of palynomorphs on the continental margin off Hokkaido Island, northwest Pacific. Mar Geol 368:58–65

Ishiwada Y (1964) Benthonic foraminifera off the Pacific coast of Japan referred to biostratigraphy of the Kazusa Group. Rep Geol Sur Japan 205:1–45

Ito H, Danišík M (2020) Dating late Quaternary events by the combined U-Pb LA-ICP-MS and (U-Th)/He dating of zircon: a case study on Omachi Tephra suite (central Japan). Terra Nova 32(2):134–140

Kaiser J, Wang KJ, Rott D, Li G, Zheng Y, Amaral-Zettler L, Arz HW, Huang Y (2019) Changes in long chain alkenone distributions and Isochrysidales group along the Baltic Sea salinity gradient. Org Geochem 127:92–103

Kajita H, Kawahata H, Wang K, Zheng H, Yang S, Ohkouchi N, Utsunomiya M, Zhou B, Zheng B (2018) Extraordinary cold episodes during the mid-Holocene in the Yangtze delta: Interruption of the earliest rice cultivating civilization. Quat Sci Rev 201:418–428

Kajita H, Nakamura H, Ohkouchi N, Harada N, Sato M, Tokioka S, Kawahata H (2020a) Genomic and geochemical identification of the long-chain alkenone producers in the estuarine Lake Takahoko, Japan: Implications for temperature reconstructions. Org Geochem 142:103980

Kajita H, Harada N, Yokoyama Y, Sato M, Ogawa N, Miyairi Y, Sawada C, Suzuki A, Kawahata H (2020b) High time-resolution alkenone paleotemperature variations in Tokyo Bay during the Meghalayan: Implications for cold climates and social unrest in Japan. Quat Sci Rev 230:106160

Kajita H, Maeda A, Utsunomiya M, Yoshimura T, Ohkouchi N, Suzuki A, Kawahata H (2021) Biomarkers in the rock outcrop of the Kazusa Group reveal palaeoenvironments of the Kuroshio region. Commun Earth Environ 2(1):1–9

Kameo K, Okada M, El-Masry M, Hisamitsu T, Saito S, Nakazato H, Ohkouchi N, Ikehara M, Yasuda H, Kitazato H, Taira A (2006) Age model, physical properties and paleoceanographic implications of the middle Pleistocene core sediments in the Choshi area, central Japan. Isl Arc 15(3):366–377

Kaneko M, Ishikawa H, Nomura M, Nakazawa T (2018) Fossil foraminiferal assemblages from the Pleistocene Shimosa Group in core GS-UR-1, Urawa, Saitama City, central Japan. Bull Geol Surv Japan 69(4):211–232

Kariya C, Hyodo M, Tanigawa K, Sato H (2010) Sea-level variation during MIS 11 constrained by stepwise Osaka Bay extensions and its relation with climatic evolution. Quat Sci Rev 29(15–16):1863–1879

Kawahata H, Yamamoto H, Ohkushi KI, Yokoyama Y, Kimoto K, Ohshima H, Matsuzaki H (2009) Changes of environments and human activity at the

Kajita *et al. Progress in Earth and Planetary Science* (2022) 9:40

Page 12 of 13

Sannai-Maruyama ruins in Japan during the mid-Holocene Hypsithermal climatic interval. Quat Sci Rev 28(9–10):964–974

Kida S, Mitsudera H, Aoki S, Guo X, Ito SI, Kobashi F, Komori N, Kubokawa A, Miyama T, Morie R, Nakamura A, Nakamura T, Nakano H, Nishigaki H, Nonaka M, Sasaki H, Sasaki YN, Suga T, Sugimoto S, Taguchi B, Takaya K, Tozuka T, Tsujimoto H, Usui N (2016) Oceanic fronts and jets around Japan: a review. In: Nakamura H, Isobe A, Minobe S, Mitsudera H, Nonaka M, Suga T (eds) "Hot Spots" in the Climate System. Springer, Tokyo, pp 1–30

Kitaba I, Hyodo M, Katoh S, Dettman DL, Sato H (2013) Midlatitude cooling caused by geomagnetic field minimum during polarity reversal. Proc Natl Acad Sci 110(4):1215–1220

Koizumi I, Yamamoto H (2010) Paleoceanographic evolution of North Pacific surface water off Japan during the past 150,000 years. Mar Micropaleontol 74(3–4):108–118

Kosugi M, Kataoka H, Hasegawa S (1991) Classification of foraminifer communities as indicators of environments in an inner bay and its application to reconstruction of paleoenvironments. Fossils 50:37–55

Lang N, Wolff EW (2011) Interglacial and glacial variability from the last 800 ka in marine, ice and terrestrial archives. Clim past 7(2):361–380

Lee KE, Clemens SC, Kubota Y, Timmermann A, Holbourn A, Yeh SW, Bae SW, Ko TW (2021) Roles of insolation forcing and CO_2 forcing on Late Pleistocene seasonal sea surface temperatures. Nat Commun 12(1):1–13

Lisiecki LE, Raymo ME (2005) A Pliocene-Pleistocene stack of 57 globally distributed benthic $\delta^{18}O$ records. Paleoceanography 20(1):PA2003

Longo WM, Dillon JT, Tarozo R, Salacup JM, Huang Y (2013) Unprecedented separation of long chain alkenones from gas chromatography with a poly (trifluoropropylmethylsiloxane) stationary phase. Org Geochem 65:94–102

Longo WM, Huang Y, Yao Y, Zhao J, Giblin AE, Wang X, Zech R, Haberzettl T, Jardillier L, Nagashima K, Sato M, Yonenobu H, Yamada K, Gotanda K, Shinozuka Y (2018) Widespread occurrence of distinct alkenones from Group I haptophytes in freshwater lakes: Implications for paleotemperature and paleoenvironmental reconstructions. Earth Planet Sci Lett 492:239–250

Lüthi D, Le Floch M, Bereiter B, Blunier T, Barnola JM, Siegenthaler U, Raynaud D, Jouzel J, Fischer H, Kawamura K, Stocker TF (2008) High-resolution carbon dioxide concentration record 650,000–800,000 years before present. Nature 453(7193):379–382

Marlowe IT, Brassell SC, Eglinton G, Green JC (1984) Long chain unsaturated ketones and esters in living algae and marine sediments. Org Geochem 6:135–141

Masuda F (2007) Paleoclimate of Interglacial Marine Isotope Stage 11 (MIS 11) from Strata in the Japanese Islands. Quat Res (Daiyonki-Kenkyu) 46(3):235–240

Matsushima Y, Ohshima K (1974) Littoral Molluscan Fauna of the Holocene Climatic Optimum (5,000–6,000 y. BP) in Japan. Quat Res (Daiyonki-Kenkyu) 13(3):135–159

Matsushima Y (1979) Littoral molluscan assemblages during the post-glacial Jomon transgression in the southern Kanto, Japan. Quat Res (Daiyonki-Kenkyu) 17:243–265

McClymont EL, Rosell-Melé A, Giraudeau J, Pierre C, Lloyd JM (2005) Alkenone and coccolith records of the mid-Pleistocene in the south-east Atlantic: implications for the $U^{K'}_{37}$ index and South African climate. Quat Sci Rev 24:1559–1572

Melles M, Brigham-Grette J, Minyuk PS, Nowaczyk NR, Wennrich V, DeConto RM, Anderson PM, Andreev AA, Coletti A, Cook TL, Haltia-Hovi E, Kukkonen M, Lozhkin AV, Rosén P, Tarasov P, Vogel H, Wagner B (2012) 28 million years of Arctic climate change from Lake El'gygytgyn, NE Russia. Science 337(6092):315–320

Milker Y, Rachmayani R, Weinkauf MFG, Prange M, Raitzsch M, Schulz M, Kučera M (2013) Global and regional sea surface temperature trends during Marine Isotope Stage 11. Clim past 9(5):2231–2252

Müller PJ, Kirst G, Ruhland G, Von Storch I, Rosell-Melé A (1998) Calibration of the alkenone paleotemperature index U37K' based on core-tops from the eastern South Atlantic and the global ocean (60 N–60 S). Geochim Cosmochim Acta 62(10):757–1772

Murray JW (2001) The niche of benthic foraminifera, critical thresholds, and proxies. Mar Micropaleontol 41(1–2):1–7

Nagashima K, Tada R, Toyoda S (2013) Westerly jet-East Asian summer monsoon connection during the Holocene. Geochem Geophys Geosyst 14(12):5041–5053

Nakagawa T, Okuda M, Yonenobu H, Miyoshi N, Fujiki T, Gotanda K, Tarasov PE, Morita Y, Takemura K, Horie S (2008) Regulation of the monsoon climate by two different orbital rhythms and forcing mechanisms. Geology 36(6):491–494

Nakamura H, Sawada K, Araie H, Suzuki I, Shiraiwa Y (2014) Long chain alkenes, alkenones and alkenoates produced by the haptophyte alga *Chrysotila lamellosa* CCMP1307 isolated from a salt marsh. Org Geochem 66:90–97

Nakamura H, Sato H (2001) Chronology of the Shimosa Group and movement of the "Kashima" uplift zone, central Japan. Quat Res (Daiyonki-Kenkyu) 40(3):251–257

Nakazawa T, Nakaszto H (2005) Depositional cycles and tephrochronology of Pleistocene Shimosa Group in central Kanto Plain, central Japan. J Geol Soc Jpn 111(2):87–93

Nakazawa T, Nakazato H (2007) Pleistocene Shimosa Group in central part of Kanto Plain, central Japan: overview. Chishitsu News 634:50–59

Nakazawa T, Nakashima R, Ueki T, Tanabe S, Oshima H, Horiuchi S (2006) Sequence stratigraphy of the Pleistocene Kioroshi Formation, Shimosa Group beneath the Omiya Upland, central Kanto Plain, central Japan. J Geol Soc Jpn 112(5):349–368

Nakazawa T, Nakazato H, Oshima H, Horiuchi S (2009) Boundary between the Kazusa and Shimosa groups beneath the central Kanto Plain: Reconstruction of MIS 12 in the GS-KS-1 core (Koshigaya, Saitama Prefecture, central Japan). J Geol Soc Jpn 115(2):49–63

Nakazawa T, Sakata K, Hongo M, Nakazato H (2017) Transition from incised valley to barrier island systems during MIS 5e in the northern Chiba area, Kanto Plain, central Japan. Quat Int 456:85–101

Nakazawa T, Tanabe S (2011) Geology of the Noda District. Quadrangle Series 1:50,000, Geol Surv Japan

Naya T, Nakayama T, Suzuki T, Sakata K, Nakazawa T (2020) Stratigraphy of the Pleistocene Tokyo Formation in the Kita-ku Central Park (Chuo-Koen) core in Kita-ku, Tokyo, central Japan. J Geol Soc Japan 126(10):575–587

Ogura H, Sato M (2001) A Bloom of *Gephyrocapsa oceanica* Kamptner in Tokyo Bay in May 1995. J Jpn Soc Water Environ 24(2):115–119

Ohkouchi N, Xu L, Reddy CM, Montluçon D, Eglinton TI (2005) Radiocarbon dating of alkenones from marine sediments: I. Isolation protocol. Radiocarbon 47(3):401–412

Okuda M, Okazaki H, Sato H (2002) Middle Pleistocene pollen assemblages and their implications for the Yabu Formation, Boso Peninsula, Central Japan. Quat Res (Daiyonki-Kenkyu) 41(5):403–412

Otto-Bliesner BL, Rosenbloom N, Stone EJ, McKay NP, Lunt DJ, Brady EC, Overpeck JT (2013) How warm was the last interglacial? New model–data comparisons. Philos Trans R Soc A:Math Phys Eng Sci 371(2001):20130097

Phillips MP, Harwood DM (2017) Marine diatom assemblage variation across Pleistocene glacial-interglacial transitions from Integrated Ocean Drilling Program Site C9001, Northwest Pacific. Palaeogeogr Palaeoclimatol Palaeoecol 483:172–187

Plancq J, Couto JM, Ijaz UZ, Leavitt PR, Toney JL (2019) Next-generation sequencing to identify lacustrine haptophytes in the Canadian Prairies: significance for temperature proxy applications. J Geophys Res: Biogeosci 124(7):2144–2158

Prahl FG, Muehlhausen LA, Zahnle DL (1988) Further evaluation of long-chain alkenones as indicators of paleoceanographic conditions. Geochim Cosmochim Acta 52(9):2303–2310

Richter N, Longo WM, George S, Shipunova A, Huang Y, Amaral-Zettler L (2019) Phylogenetic diversity in freshwater-dwelling Isochrysidales haptophytes with implications for alkenone production. Geobiology 17(3):272–280

Sagawa T, Nagahashi Y, Satoguchi Y, Holbourn A, Itaki T, Gallagher SJ, Saavedra-Pellitero M, Ikehara K, Irino T, Tada R (2018) Integrated tephrostratigraphy and stable isotope stratigraphy in the Japan Sea and East China Sea using IODP Sites U1426, U1427, and U1429, Expedition 346 Asian Monsoon. Prog Earth Planet Sci 5(1):1–24

Salacup JM, Farmer JR, Herbert TD, Prell WL (2019) Alkenone paleothermometry in coastal settings: Evaluating the potential for highly resolved time series of sea surface temperature. Paleoceanogr Paleoclimatol 34(2):164–181

Sampe T, Xie SP (2010) Large-scale dynamics of the Meiyu-Baiu rainband: environmental forcing by the westerly jet. J Clim 23(1):113–134

Sawada K, Handa N, Shiraiwa Y, Danbara A, Montani S (1996) Long-chain alkenones and alkyl alkenoates in the coastal and pelagic sediments of the northwest North Pacific, with special reference to the reconstruction of *Emiliania huxleyi* and *Gephyrocapsa oceanica* ratios. Org Geochem 24(8–9):751–764

Sixth Assessment Report (2021) The Intergovernmental Panel on Climate Change (IPCC)

Suzuki H (2002) Underground geological structure beneath the Kanto Plain, Japan. Report of the National Research Institute for Earth Science and Disaster Resilience 63:1–19

Tada R, Murray RW (2016) Preface for the article collection 'Land–Ocean Linkages under the Influence of the Asian Monsoon.' Prog Earth Planet Sci 3(1):1–5

Tada R, Irino T, Ikehara K, Karasuda A, Sugisaki S, Xuan C, Sagawa T, Itaki T, Kubota Y, Lu S, Seki A, Murray RW, Alvarez-Zarikian C, Anderson WT Jr, Bassetti M, Brace BJ, Clemens SC, da Costa Gurgel MH, Dickens GR, Dunlea AG, Gallagher SJ, Giosan L, Henderson ACG, Holbourn AE, Kinsley CW, Lee GS, Lee KE, Lofi J, Lopes CIDD, Saavedra-Pellitero M et al (2018) High-resolution and high-precision correlation of dark and light layers in the Quaternary hemipelagic sediments of the Japan Sea recovered during IODP Expedition 346. Progr Earth Planet Sci 5(1):1–10

Tarasov PE, Nakagawa T, Demske D, Österle H, Igarashi Y, Kitagawa J, Mokhova L, Bazarova V, Okuda M, Gotanda K, Miyoshi N, Fujiki T, Takemura K, Yonenobu H, Fleck A (2011) Progress in the reconstruction of Quaternary climate dynamics in the Northwest Pacific: A new modern analogue reference dataset and its application to the 430-kyr pollen record from Lake Biwa. Earth Sci Rev 108(1–2):64–79

Theroux S, D'Andrea WJ, Toney J, Amaral-Zettler L, Huang Y (2010) Phylogenetic diversity and evolutionary relatedness of alkenone-producing haptophyte algae in lakes: implications for continental paleotemperature reconstructions. Earth Planet Sci Lett 300(3–4):311–320

Thomas ZA, Jones RT, Turney CS, Golledge N, Fogwill C, Bradshaw C, Menviel L, McKay NP, Bird N, Palmer J, Kershaw P, Wilmshurst J, Muscheler R (2020) Tipping elements and amplified polar warming during the Last Interglacial. Quat Sci Rev 233:106222

Tierney JE, Tingley MP (2018) BAYSPLINE: A new calibration for the alkenone paleothermometer. Paleoceanogr Paleoclimatol 33(3):281–301

Tokuhashi S, Endo S (1984) Geology of the Anesaki District. Quadrangle Series 1:50,000, Geol Surv Japan

Tokuhashi S, Kondo Y (1989) Sedimentary cycles and environments in the middle-late Pleistocene Shimosa Group, Boso Peninsula, central Japan. J Geol Soc Jpn 95(12):933–951

Tsukamoto S, Murray AS, Huot S, Watanuki T, Denby PM, Bøtter-Jensen L (2007) Luminescence property of volcanic quartz and the use of red isothermal TL for dating tephras. Radiat Meas 42(2):190–197

Turney CS, Jones RT, McKay NP, Van Sebille E, Thomas ZA, Hillenbrand CD, Fogwill CJ (2020) A global mean sea surface temperature dataset for the Last Interglacial (129–116 ka) and contribution of thermal expansion to sea level change. Earth Syst Sci Data 12(4):3341–3356

Tzedakis PC, Raynaud D, McManus JF, Berger A, Brovkin V, Kiefer T (2009) Interglacial diversity. Nat Geosci 2(11):751–755

Tzedakis PC, Wolff EW, Skinner LC, Brovkin V, Hodell DA, McManus JF, Raynaud D (2012) Can we predict the duration of an interglacial? Clim past 8(5):1473–1485

Uemura R, Motoyama H, Masson-Delmotte V, Jouzel J, Kawamura K, Goto-Azuma K, Fujita S, Kuramoto T, Hirabayashi M, Miyake T, Ohno H, Fujita K, Abe-Ouchi A, Iizuka Y, Horikawa S, Igarashi M, Suzuki K, Suzuki T, Fujii Y (2018) Asynchrony between Antarctic temperature and CO_2 associated with obliquity over the past 720,000 years. Nat Commun 9(1):1–11

Volkman JK, Eglinton G, Corner EDS, Sargent JR (1980) Novel unsaturated straight-chain C37–C39 methyl and ethyl ketones in marine sediments and a coccolithophore *Emiliania huxleyi*. Phys Chem Earth 12:219–227

Wang KJ, Huang Y, Majaneva M, Belt ST, Liao S, Novak J, Kartzinel TR, Herbert TD, Richter N, Cabedo-Sanz P (2021) Group 2i Isochrysidales produce characteristic alkenones reflecting sea ice distribution. Nat Commun 12:15

Yamamoto M, Oba T, Shimamune J, Ueshima T (2004) Orbital-scale anti-phase variation of sea surface temperature in mid-latitude North Pacific margins during the last 145,000 years. Geophys Res Lett 31(16)

Yao Y, Zhao J, Vachula RS, Liao S, Li G, Pearson EJ, Huang Y (2022) Phylogeny, alkenone profiles and ecology of Isochrysidales subclades in saline lakes: implications for paleosalinity and paleotemperature reconstructions. Geochim Cosmochim Acta 317:472–487

Yin QZ, Berger A (2010) Insolation and CO_2 contribution to the interglacial climate before and after the Mid-Brunhes Event. Nat Geosci 3(4):243–246

Young JR, Geisen M, Cros L, Kleijne A, Sprengel C, Probert I, Østergaard JB (2003) A guide to extant coccolithophore taxonomy. J Nannoplank Res 1:1–132

Zheng Y, Heng P, Conte M, Vachula RS, Huang Y (2019) Systematic chemotaxonomic profiling and novel paleotemperature indices based on alkenones and alkenoates: Potential for disentangling mixed species input. Org Geochem 128:26–41

Publisher's Note